SUPERCONDUCTIVITY AND MAGNETISM IN METALLIC SUPERLATTICES*

IVAN K. SCHULLER AND CHARLES M. FALCO

Solid State Science Division, Argonne National Laboratory, Argonne, IL 60439 (U.S.A.)

The preparation, structural and physical properties (superconductivity and magnetism) of metallic superlattices prepared by a sputtering technique developed by us are presented. X-ray diffraction, ion mill Auger and ion scattering spectroscopy, superconducting T_c and H_c values, as well as magnetization measurements, are described.

1. INTRODUCTION

Research on metallic superlattices and layered metals is at a much earlier stage of development than that on similar semiconducting structures. In spite of the fact that metallic systems were produced earlier, until very recently they only received attention by a few groups[1-6]. Major steps have recently been taken towards improving the structural quality (crystal size, sharpness of interface etc.) of metallic superlattices where it is now possible to contemplate the development of high quality samples in the near future.

2. PREPARATION TECHNIQUES

The experimental preparation techniques for metallic superlattices can be divided into two main categories: evaporation and sputtering. Many single-layer metals have been deposited epitaxially onto a large variety of substrates using both techniques (see, for example, various chapters in ref. 7). The deposition rates, the substrate temperature and the residual gases are critical for both evaporation and sputtering. For sputtering, the distance of the substrate from the sputtering gun and the sputtering gas pressure have major effects on the quality of the epitaxial films.

The sputtered materials described in the present paper have been prepared using a technique developed by us[5,6]. Two high rate magnetron sputtering guns and one r.f. sputter gun are symmetrically placed in a high vacuum system (base pressure, about 8×10^{-8} Torr). The sputtering guns are shielded by several baffles to eliminate

---

any overlap of the sputtered beams completely. The rates are controlled by regulating the power to the guns and are monitored using quartz crystal oscillators. In fact, the rates are highly stable over the period of a number of depositions, so that active feedback control of the guns is not necessary. The single-crystal substrates (90°- or 0°-oriented Al_2O_3, mica or MgO) are located on a motor-driven platform whose temperature is controlled using a non-contact temperature sensor and a quartz lamp heater in a feedback loop. This system allows us to vary the substrate temperature from room temperature to approximately 400 °C with an accuracy of ± 2 °C. As for thermally evaporated films, substrate temperature control is essential for the production of epitaxial sputtered films. For example, the Laue patterns of silver films grown on mica at room temperature, at 107 °C and at 278 °C respectively show rings only, both rings and spots, and spots only. By proper regulation of the sputtering rates and the rotation speed of the platform, layers ranging in thickness from 2 Å to greater than 1 μm have been reproducibly prepared.

We feel that an advantage of sputtering over thermal deposition techniques is that by varying the sputtering pressure (typically argon at 0.5–20 mTorr) as well as the target-to-substrate distance it is possible to control the energy distribution of particles arriving at the substrate. We have performed a calculation using typical parameters encountered in sputtering which demonstrates this[8]. We find that, as the particles travel through the gas, the energy distribution sharpens and moves to lower energies, finally attaining a Boltzmann distribution characteristic of the gas temperature. A comparison (Fig. 1) of the final energy distributions of sputtered and evaporated copper normalized to the same total flux shows the sputtered distribution to be sharper with a peak energy lower than that of evaporated copper. This difference is even more pronounced for more refractory materials, such as niobium.

3. STRUCTURE

Multilayers of Nb/Cu, Nb/Ti, Nb/Ni and Ni/Ag have been prepared using the technique described above. Nb/Cu has been most extensively studied to date, so our discussion of structural characteristics will emphasize this material. Similar information has been obtained on our other metallic superlattice samples. Ion mill
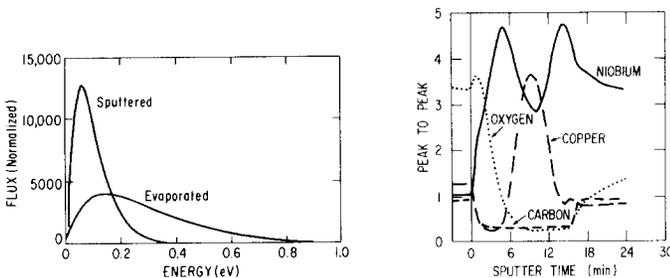

Fig. 1. Comparison of calculated final energy distributions for sputtered and thermally evaporated copper.

Fig. 2. Dependence of peak-to-peak Auger amplitudes for niobium, copper, oxygen and carbon as a function of ion milling time (distance into sample) for an Nb(65 Å)/Cu(65 Å) sample.

Auger spectroscopy as well as ion mill ion scattering spectroscopy (ISS) have been performed to depth profile the chemical composition of the samples. Figure 2 shows the results of an ion mill Auger study of the chemical composition as a function of depth for an Nb(65 Å)/Cu(65 Å) multilayer. It should be noted that the surface layer is niobium and that the surface of the sample is considerably contaminated by oxygen and carbon. After about 40 Å (about 6 min) of ion milling with 1 keV argon ions, both the oxygen and the carbon peaks are undetectable, indicating that only the surface of the sample is contaminated. When the sample is milled, the peaks due to copper and niobium oscillate out of phase as expected for a layered material.

Ideally it would be desirable to obtain composition information down to the atomic level so that the nature of the interface between layers can be studied. The difficulty with ion mill Auger spectroscopy for this purpose is twofold. The escape depth for the Auger electrons is energy dependent but even in the most favorable case is about 20 Å. Therefore, the Auger signal is only indicative of the chemical composition averaged over at least a 20 Å depth, *i.e.* approximately eight to ten atomic layers. An additional problem is that the process of ion milling causes significant intermixing of the layers as well as cratering which tends to destroy the layered structure. In order to obviate the finite escape depth problem inherent in the Auger measurements, ISS measurements have also been performed. Figure 3 shows the niobium signal intensity for the Nb(65 Å)/Cu(65 Å) sample as a function of ion milling time as determined using 1 keV ^{20}Ne$^+$ ions. For the first layer, an essentially 100% composition modulation is observed; however, the intermixing problems caused by the ion milling can clearly be seen to distort the results for subsequent
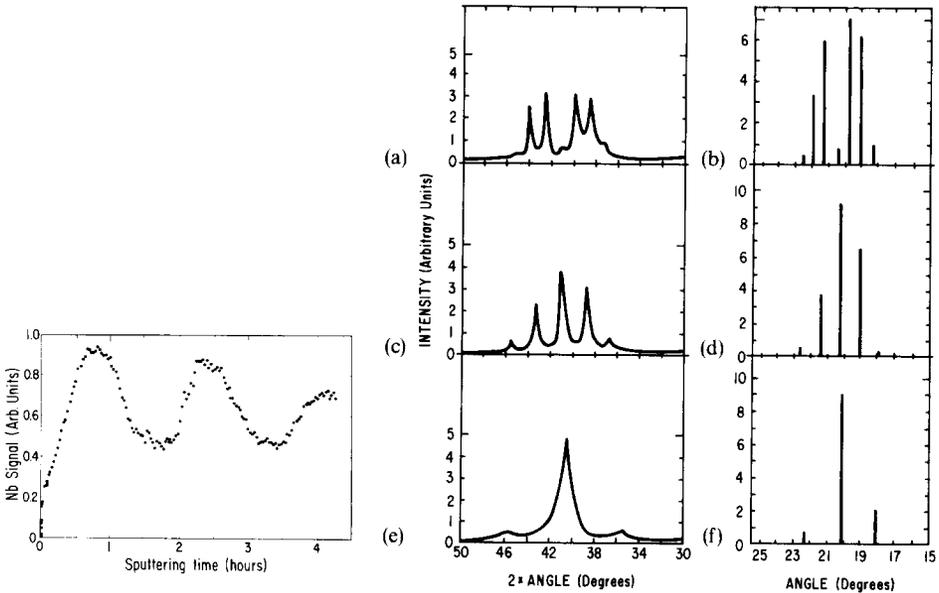

Fig. 3. Dependence of niobium ISS amplitude as a function of ion milling time (distance into sample) for an Nb(65 Å)/Cu(65 Å) sample.

Fig. 4. Measured and calculated X-ray diffraction patterns for a series of Nb/Cu samples of different layer thicknesses ($\lambda/2$): (a), (b) 34 Å; (c), (d) 22 Å; (e), (f) 10 Å.

layers. The conclusions from these measurements are that the chemical composition of these materials is modulated but that ion milling techniques are not useful for layer thicknesses below about 40 Å.

To study the crystal structure we have performed standard θ–2θ X-ray scattering on a variety of Nb/Cu, Nb/Ti and Ni/Ag samples[6]. Since the X-ray momentum transfer is perpendicular to the layers, this measurement is only sensitive to structural changes perpendicular to the layers. A one-dimensional model calculation on the assumption of 100% composition modulation indicates that characteristic peaks should arise because of scattering by the superlattice planes. The layer thickness ($\lambda/2$) is given by the simple formula

$$\lambda = \frac{\lambda_{\mathrm{X}}}{2} \frac{1}{\sin \theta_i - \sin \theta_{i+1}} \tag{1}$$

where λ_{X} is the X-ray wavelength and i and $i+1$ refer to adjacent diffraction peaks. Figure 4 shows the measured and calculated X-ray intensities *versus* 2θ for a series of Nb/Cu samples. We should stress that the existence of a large number of superlattice reflections implies that the position of atomic planes perpendicular to the layers is correlated. As in any anisotropic system, several coherence lengths can be defined. In particular, the X-ray measurement described above gives a lower limit on the coherence of the Cu/Nb superlattice in the z direction (perpendicular to the layers) of about ten superlattice wavelengths.

4. SUPERCONDUCTIVITY

An area of much promise for the observation of effects due to the imposition of a superlattice is the phenomenon of superconductivity. In this case the relevant length is the superconductive coherence length (16 000 Å for aluminum, 380 Å for niobium etc.), which is long compared with the layer thicknesses which can already be reliably prepared.

We have made both inductive and resistive measurements of the superconductive T_c values of a series of Nb/Cu samples ranging in layer thickness[9] from 5 to 5000 Å. In all cases the total sample thickness was about 1 μm. The T_c values measured inductively or resistively on these samples are in close agreement. The resistive transition width (about 60 mK) in these samples is quite narrow, indicating the absence of a large distribution of inhomogeneities.

The superconducting transition temperatures are affected by changes in layer thickness; for Nb/Cu the transition temperatures start at the 9 K value characteristic of niobium (prepared under identical conditions) and decrease monotonically with decreasing layer thickness (Fig. 5). Above 200 Å, the changes in T_c *versus* layer thickness can be explained, with no adjustable parameters, by proximity effect theories. Below 200 Å, these data can also be explained by proximity effect theories; however, it is also necessary to invoke a decrease in the transition temperature of niobium as the layer thickness is reduced. Thus for the thin layers (less than 200 Å) the T_c value for niobium is obtained as a parameter. The decrease in the T_c value for niobium inferred from these measurements is in qualitative agreement with measurements of T_c values for thin single-layer niobium films[10] and also radiation-damaged thick niobium films[11]. Such decreases in T_c for niobium have been previously ascribed[12] to changes in the density N_0 of states at the Fermi surface.

Figure 6 shows the critical field for an Nb/Cu superlattice of 10 Å layer spacing. The anisotropy is similar to that observed in the layered compounds, *i.e.* the parallel critical field $H_\parallel$ is larger than the perpendicular critical field $H_\perp$. Since the layers are so strongly coupled, the explanation has to lie elsewhere than in the Josephson weak-coupled layered model (see ref. 13) as advanced by Lawrence and Doniach[14]. An alternative explanation may lie in the anisotropy of the band structure similar to Nb_3Pt which shows anisotropic critical fields arising from anisotropic electron masses[15]. However, any comparison between theory and experiment will have to be done using detailed band structure calculations for the particular system under study. We have extensive measurements in progress in order to help to answer this problem.
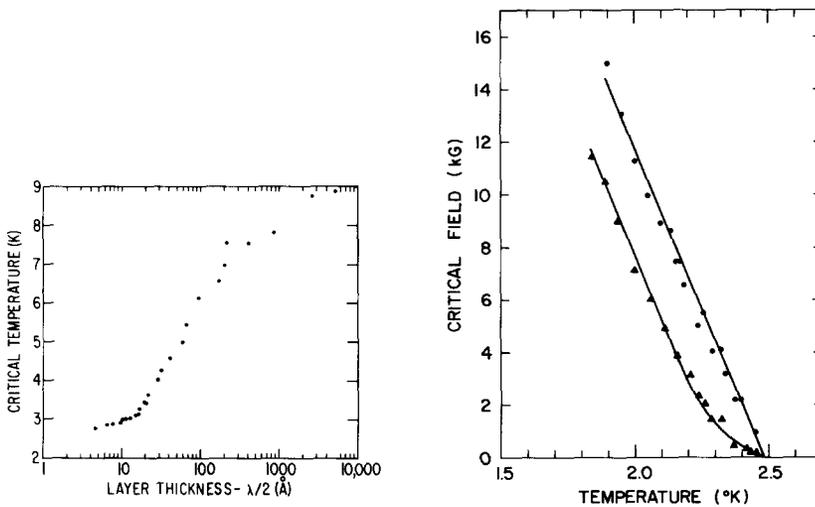

Fig. 5. Measured superconducting transition temperature *vs.* layer thickness ($\lambda/2$) for a series of Nb/Cu samples.

Fig. 6. Superconducting critical fields parallel and perpendicular to the layers for an Nb(10 Å)/Cu(10 Å) sample ($\lambda/2 = 10$ Å): ●, $H_\parallel$; ▲, $H_\perp$.

5. MAGNETISM

Magnetism is another phenomenon in which superlattice effects might be observed. We are at present studying the growth of several possible magnetic superlattices. To date, we have obtained measurements (in collaboration with J. B. Ketterson and J. Q. Zheng) on partially layered Cu/Ni samples[16]. In this case the materials are mutually soluble so that the composition can be modulated around some average value but complete layering is not obtained.

Cu/Ni samples were prepared on mica substrates using a dual-electron-beam-gun evaporator rather than by sputtering. Structural studies demonstrate that these Cu/Ni samples are preferentially oriented along the (111) direction. Laue diffraction studies also show that the material is crystalline in the *x–y* plane.

We have measured the magnetization of Cu/Ni over a wide magnetic field (0–10 kG) and temperature (5–350 K) range. These results are shown in Figs. 7 and 8.

The data show magnetizations reduced from that of pure nickel in agreement with neutron scattering experiments and band structure calculations. The saturation magnetization varies with composition amplitude and is independent of modulation wavelength. The Curie temperature is amplitude independent and decreases with decreasing wavelength. The magnetic field dependence of the magnetization implies that there is only a small magnetostrictive term, indicating the absence of large strains in this material. The temperature dependence of the saturation magnetization indicates a Curie point independent of modulation amplitude. All the observed properties are consistent with the idea that the properties of Cu/Ni samples are determined by thin film effects rather than by any influence of a superlattice. Clearly, more ideal magnetic materials are required, and we are working on this problem.
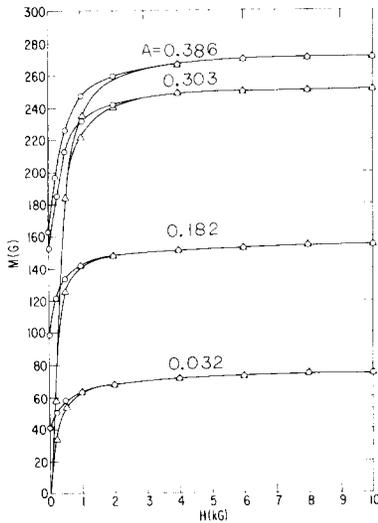

Fig. 7. Magnetization *vs.* *H* for a 60%Cu/40%Ni sample with $\lambda/2 = 15.2$ Å (four different composition modulation amplitudes obtained from successive annealing are shown): $\triangle$, increasing *H*; $\bigcirc$, decreasing *H*.
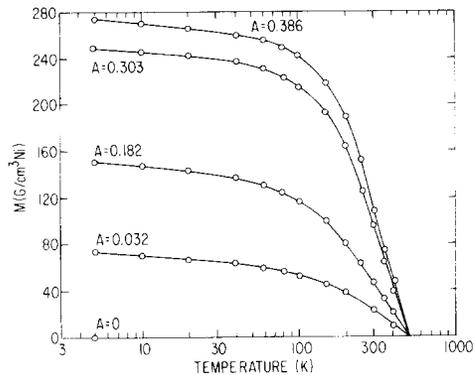
Fig. 8. Temperature dependence of the saturation magnetization for the sample shown in Fig. 7.

6. SUMMARIZING REMARKS

Compositional (ion mill Auger spectroscopy and ISS) and structural studies show that metallic superlattices can be prepared by sputtering. Calculations indicate that this in part may be due to the role that the sputtering gas plays in determining the energy distribution of atoms at the substrate. Nb/Cu samples have been prepared which show large-range structural coherence (about 10λ) perpendicular to the layers. Superconducting T_c and anisotropic H_c values have been obtained which are indicative of the layered nature of these materials. Work is under way to provide equivalent quality superlattices using magnetic materials.

REFERENCES

1　J. E. Hilliard, in J. M. Cowley, J. B. Cohen, M. B. Salamon and B. J. Wuensch (eds.), *Modulated Structures—1979*, American Institute of Physics, New York, 1979, p. 407.
2　M. Strongin, O. F. Kammerer, J. E. Crow, R. D. Parks, D. H. Douglas, Jr., and M. A. Jensen, *Phys. Rev. Lett.*, *21* (1968) 1320.
3　M. R. Beasley, in D. U. Gubser, T. L. Francavilla, J. R. Leibowitz and S. A. Wolf (eds.), *Inhomogeneous Superconductors—1979*, American Institute of Physics, New York, 1980, p. 186.
4　J. B. Ketterson, *Proc. 110th Annu. Meet. of the Metallurgical Society of AIME*, Metallurgical Society of AIME, New York, 1981, p. 70.
5　I. K. Schuller and C. M. Falco, in D. U. Gubser, T. L. Francavilla, J. R. Leibowitz and S. A. Wolf (eds.), *Inhomogeneous Superconductors—1979*, American Institute of Physics, New York, 1980, p. 197.
6　I. K. Schuller, *Phys. Rev. Lett.*, *44* (1980) 1597.
7　J. W. Matthews (ed.), *Epitaxial Growth*, Academic Press, New York, 1975.
8　K. Meyer, I. K. Schuller and C. M. Falco, *J. Appl. Phys.*, *52* (1981) 6608.
9　I. Banerjee, Q. S. Yang, C. M. Falco and I. K. Schuller, *Solid State Commun.*, (1982), in the press.
10　S. A. Wolf, J. J. Kennedy and M. Nisenoff, *J. Vac. Sci. Technol.*, *13* (1976) 145.
11　H. Lutz, H. Weisman, M. Gurevitch, A. Goland, O. F. Kammerer and M. Strongin, in D. H. Douglas (ed.), *Superconductivity in d and f Band Metals, Proc. 2nd Rochester Conf.*, Plenum, New York, 1976, p. 535.
12　C. M. Varma and R. C. Dynes, in D. H. Douglas (ed.), *Superconductivity in d and f Band Metals, Proc. 2nd Rochester Conf.*, Plenum, New York, 1976, p. 507.
13　R. A. Klemm, A. Luther and M. R. Beasley, *Phys. Rev. B*, *12* (1975) 877, and references cited therein.
14　W. Lawrence and S. Doniach, in E. Kanda (ed.), *Proc. 12th Int. Conf. on Low Temperature Physics*, Academic Press of Japan, Kyoto, 1971, p. 361.
15　P. Entel and M. Peter, *J. Low Temp. Phys.*, *22* (1976) 613.
16　J. Q. Zheng, C. M. Falco, J. B. Ketterson and I. K. Schuller, *Appl. Phys. Lett.*, *38* (1981) 424; *J. Appl. Phys.*, (1982), in the press.